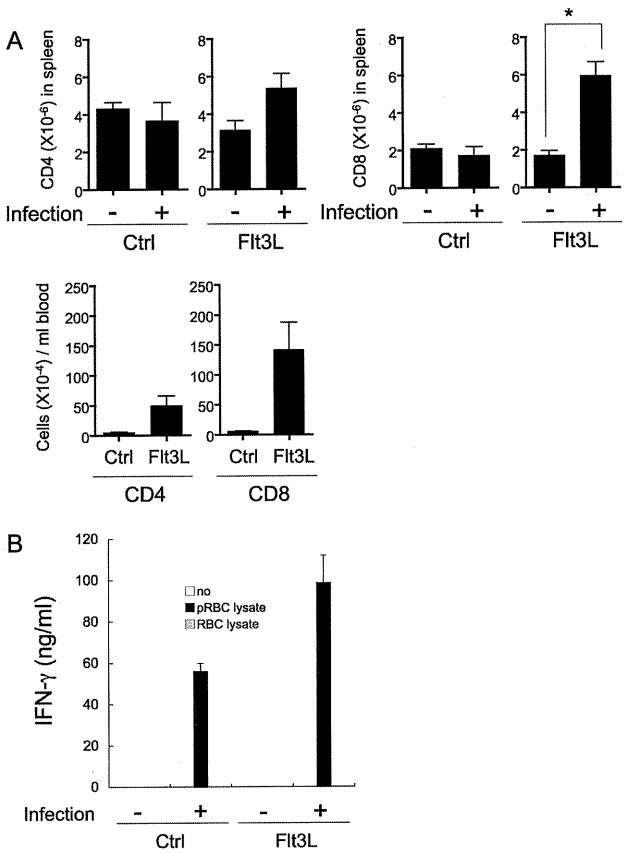

FIG. 3. The number of $CD8^+$ T cells was markedly increased in Flt3L-treated mice after infection with *P. berghei* ANKA. (A) Mice were either left untreated or were treated with Flt3L; then they were either left uninfected or infected with *P. berghei* ANKA for 5 days. Spleen cells and peripheral blood lymphocytes were stained for CD4, CD8, and TCR, and the numbers of $CD4^+$ and $CD8^+$ T cells were calculated. *, $P < 0.05$ by the Mann-Whitney test. (B) $CD8^+$ T cells were cultured in triplicate wells in the presence of DCs pulsed with nothing (open bars), a pRBC lysate (filled bars), or an RBC lysate (shaded bars) for 48 h, and the levels of IFN-γ were determined by ELISA. The experiments were repeated twice, and representative data are shown.

significantly induced in $CD4^+$ T cells upon *P. berghei* ANKA infection (Fig. 4A). The majority of $CD11c^+$ $CD8^+$ T cells coexpressed CD44, suggesting that they were recently activated effector T cells (Fig. 4B). CD11c is a well-known marker of DCs, but it was previously reported that some activated $CD8^+$ T cells express CD11c (4, 13, 18). We sorted $CD11c^+$ $CD8^+$ and $CD11c^-$ $CD8^+$ T cells from the spleens of *P. berghei* ANKA-infected mice, and we stimulated them with an anti-TCR MAb *in vitro*. $CD11c^+$ $CD8^+$ T cells produced IFN-γ at a level much higher than that of $CD11c^-$ $CD8^+$ T cells, confirming that they were primed T cells (data not shown).

Focusing on $CD11c^+$ $CD8^+$ T cells, we examined their expression of other activation-associated molecules and the chemokine receptor CXCR3, which was previously reported to be instrumental to ECM pathogenesis (Fig. 4B and C) (6, 24, 37). The expression of CD44 and CXCR3 on $CD11c^+$ $CD8^+$ T cells was similarly upregulated in both Flt3L-treated and untreated mice. However, the expression of CD25, CD137, and granzyme B in $CD11c^+$ $CD8^+$ T cells from Flt3L-treated mice was lower than their expression in $CD11c^+$ $CD8^+$ T cells from untreated mice (Fig. 4C). These results suggest that the activation status of $CD8^+$ T cells in Flt3L-treated mice was distinct from that in untreated mice during infection with *P. berghei* ANKA.

Next, cells sequestered in the brains of *P. berghei* ANKA-infected mice 6 days after infection were examined (Fig. 4D). The numbers of both $CD8^+$ and $CD4^+$ T cells increased dramatically in both Flt3L-treated and untreated mice after *P. berghei* ANKA infection. No significant difference in the number of brain-sequestered T cells between Flt3L-treated and untreated mice was found. The majority of brain-sequestered $CD8^+$ T cells expressed CD44 and CD11c, indicating that they were activated T cells. The levels of CD44 expression were similar in Flt3L-treated and untreated mice, while CD11c expression levels were slightly lower in brain-sequestered $CD8^+$ T cells from Flt3L-treated mice than in those from untreated mice. To gain insight into the function of these brain-sequestered $CD8^+$ T cells, the expression of IFN-γ and granzyme B was evaluated by intracellular staining after stimulation with an anti-TCR MAb (Fig. 4E). The proportions of $CD8^+$ T cells that produced IFN-γ alone or both IFN-γ and granzyme B were lower in Flt3L-treated mice than in the control group. Taken together, these results suggest that the activation status of brain-sequestered $CD8^+$ T cells in Flt3L-treated mice is lower than that for untreated mice. Since sequestration of both $CD8^+$ T cells and pRBC is required for the pathogenesis of ECM, we also examined the number of pRBC in the brains of Flt3L-treated mice (Fig. 4F). The number of brain-sequestered pRBC was strikingly reduced in Flt3L-treated mice, consistent with protection from lethal ECM.

Roles of Treg and granulocytes in Flt3L-treated mice. To investigate the possible role of regulatory $CD4^+$ T cells (Treg) in the differential activation of $CD8^+$ T cells in Flt3L-treated mice, we first examined the number of $Foxp3^+$ Treg (Fig. 5A). The proportion of Treg in the spleens of Flt3L-treated mice was higher than the proportion in untreated mice, consistent with a previous report (35). However, the proportion of Treg did not change significantly after infection with *P. berghei* ANKA in either control or Flt3L-treated mice. Therefore, Treg did not proliferate preferentially in Flt3L-treated mice during *P. berghei* ANKA infection. We next examined IFN-γ production by $CD4^+$ T cells and found that $CD4^+$ T cells from Flt3L-treated and untreated mice produced similar levels of IFN-γ in response to an anti-TCR Ab (Fig. 5B). Since $CD4^+$ T cells from Flt3L-treated and untreated mice contained similar levels of $FoxP3^+$ Treg after infection with *P. berghei* ANKA, it is unlikely that the functions of Treg in these two groups of mice are significantly different. Therefore, it is unlikely that the differences in $CD8^+$ T cells between Flt3L-treated and untreated mice are due to differences in Treg.

Treatment of mice with Flt3L increased the number of granulocytes and DCs in the spleen (Fig. 1B). The role of granulocytes in the pathogenesis of malaria has been evaluated previously; two studies reported that the depletion of granulocytes by antibody treatment did not significantly affect the level of parasitemia but prevented the development of ECM (7, 30), while one study reported that granulocyte depletion in the effector phase did not affect ECM pathogenesis (3). Thus, we

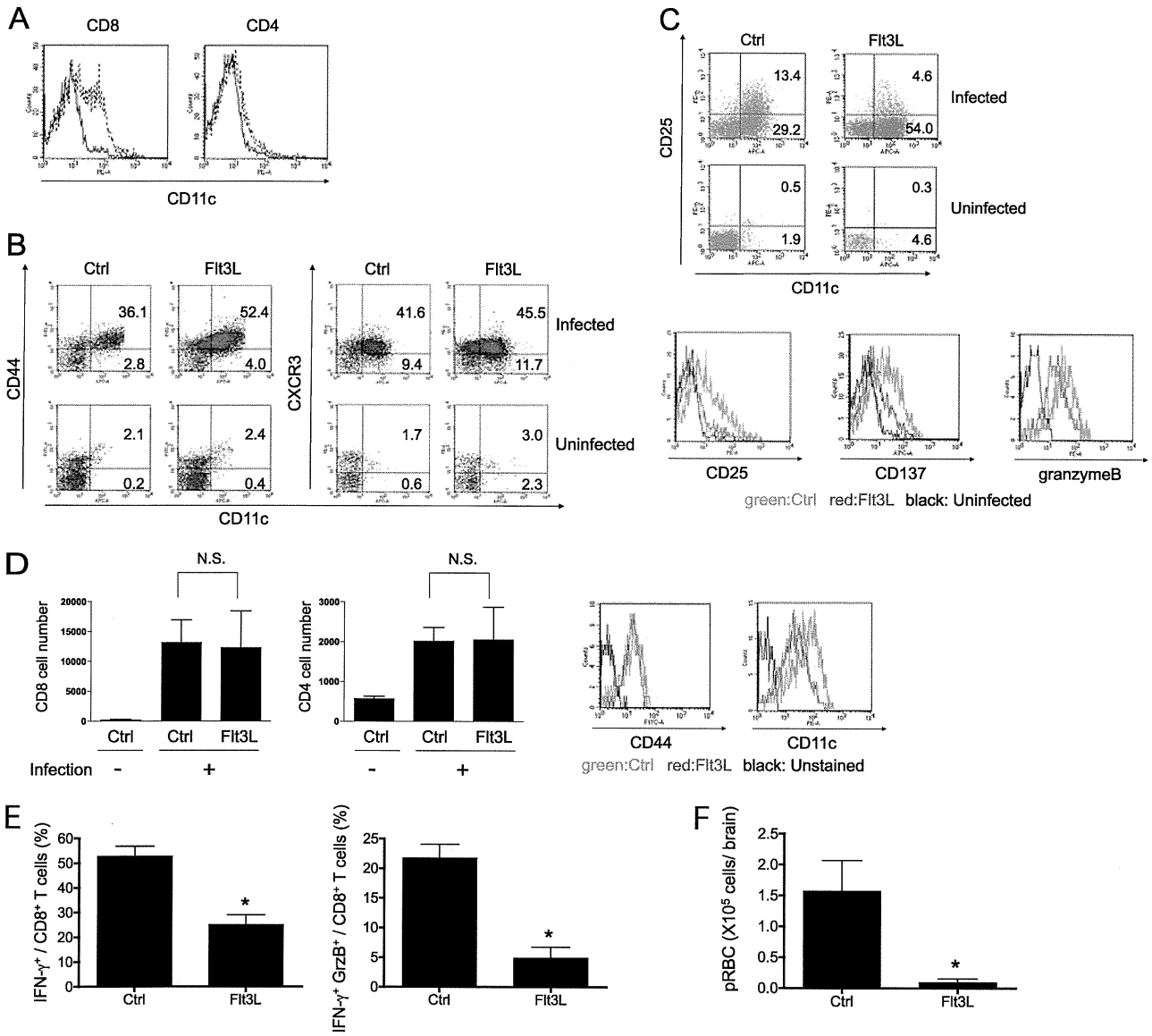

FIG. 4. The activation phenotype of $CD8^+$ T cells from Flt3L-treated mice after *P. berghei* ANKA infection was distinct from that of untreated mice. (A) B6 mice were either left uninfected (solid lines) or infected with *P. berghei* ANKA (dotted lines). Five days later, spleen cells were stained for CD11c, TCR, CD8, and CD4, and the expression of CD11c on $CD8^+$ and $CD4^+$ T cells was examined. (B and C) Mice were either left untreated or treated with Flt3L, after which they were either left uninfected or infected with *P. berghei* ANKA, and splenocytes were stained with MAbs 5 days after infection. The dot plots demonstrate the expression of CD11c, CD44, CXCR3 (B), and CD25 (C) on $CD8^+$ T cells. The number in each quadrant represents the proportion of cells within the region. The histograms (C) demonstrate the expression of CD25, CD137, and granzyme B on splenic $CD11c^+$ $CD8^+$ T cells from untreated (green) and Flt3L-treated (red) mice 5 days after *P. berghei* ANKA infection or from uninfected, untreated mice (black). Ctrl, control. (D) (Left) Brain-sequestered cells were isolated from uninfected and infected mice (3 mice/group), and total cell numbers were quantified. Cells were stained for CD45, Ter119, CD4, CD8, and TCR, and the numbers of $CD8^+$ and $CD4^+$ T cells ($CD45^+$ $Ter119^-$ TCR^+) were calculated and are shown as means ± SD. N.S., no significant difference between the Ctrl and Flt3L groups by the Mann-Whitney test. (Right) Expression of CD44 and CD11c on brain-sequestered $CD8^+$ T cells from untreated (green) and Flt3L-treated (red) B6 mice after 6 days of strain ANKA infection. The black line represents control unstained brain-sequestered $CD8^+$ T cells. (E) Brain-sequestered $CD8^+$ T cells were stimulated with an anti-TCR MAb, and the expression of IFN-γ and granzyme B (GrzB) was determined using intracellular staining. *, $P < 0.05$ by the Mann-Whitney test. (F) Mice (3 per group) were either left untreated or treated with Flt3L and were infected with *P. berghei* ANKA. After 6 days, brain-sequestered pRBC were counted. *, $P < 0.05$ by the Mann-Whitney test. The experiments were repeated twice, and representative data are shown.

evaluated the role of granulocytes in the inhibition of ECM and parasitemia (Fig. 6). Depletion of granulocytes with an anti-Gr1 MAb (>99%) prior to infection did not significantly affect the levels of parasitemia in either control or Flt3L-treated mice and did not alter the inhibitory effect of Flt3L on the development of ECM. Therefore, we concluded that the inhibition of ECM by Flt3L treatment was not due to an increase in the number of granulocytes.

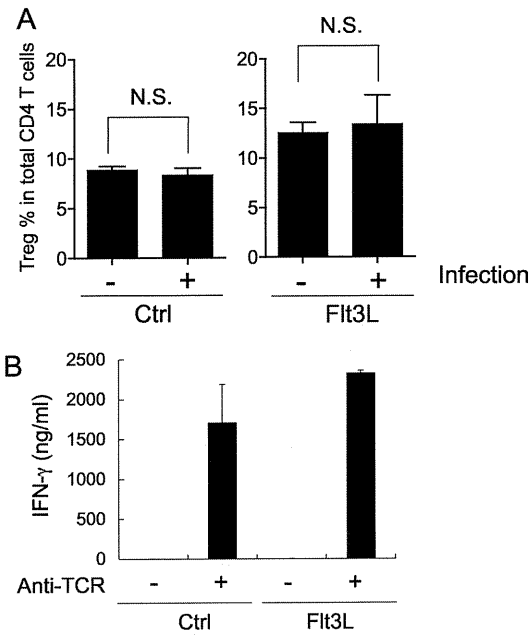

FIG. 5. Treg are unlikely to be involved in the inhibition of $CD8^+$ T cell activation in Flt3L-treated mice after *P. berghei* ANKA infection. (A) Untreated (3 per group) and Flt3L-treated (4 per group) mice were either left uninfected or infected with *P. berghei* ANKA. After 5 days, splenocytes were stained for CD4, CD25, and Foxp3. The ratio of Treg ($CD4^+$ $CD25^+$ $Foxp3^+$) within $CD4^+$ T cells was expressed as the mean ± SD for each group. N.S., no significant difference. (B) Five days after infection, $CD4^+$ splenic T cells were stimulated with a plate-bound anti-TCR MAb, and their IFN-γ production was determined by a quadruplicate ELISA. The experiments were repeated twice, and representative data are shown.

DISCUSSION

DCs are critical immune cells in both innate and adaptive immunity. During infection with malaria parasites, DCs take up *Plasmodium*-infected RBC and can induce the initiation of protective immune responses. To better understand the role of DCs during malaria infection, we have taken the approach of expanding DCs with Flt3L *in vivo* prior to infection with *P. berghei* ANKA. Flt3L was effective in augmenting protective innate immune responses during the early phase of *P. berghei* ANKA infection, and it induced altered activation of $CD8^+$ T cells, culminating in prevention of ECM.

We employed the hydrodynamic method to induce Flt3L *in vivo*, and we observed an increase in the number of DCs in the spleen. The proportion of $CD8^+$ DCs was increased to more than 50% of all DCs, consistent with the report from a previous study that used an adenoviral vector expressing recombinant Flt3L (23). These DCs expressed MHC and costimulatory molecules at levels similar to those of controls and were superior in cross-presenting malaria antigens to specific $CD8^+$ T cells, as previously reported (19). After infection of Flt3L-treated mice with *P. berghei* ANKA, a significant reduction in the level of parasitemia was observed during the initial period of the infection, suggesting that Flt3L-treated mice were more protected than untreated mice. We speculate that this initial protective response was due mainly to enhancement of innate immunity, since we observed a similar reduction in parasitemia levels in Flt3L-treated $Rag2^{-/-}$ mice, which lack both T and B cells. We suspect that the expansion of DCs contributes to reduced parasitemia through DC phagocytosis of pRBC. Granulocytes may be less involved, since parasitemia levels were not significantly increased in mice depleted of granulocytes. This protection, however, was not long-lasting, and parasitemia levels rose in Flt3L-treated mice until they succumbed to death.

To investigate the mechanisms that lead to the prevention of ECM by Flt3L treatment, we studied the effects of Flt3L treatment on T cells, since T cells play an instrumental role in the pathogenesis of ECM. We first observed the marked increase in the number of $CD8^+$ T cells in the spleens of Flt3L-treated mice after infection with *P. berghei* ANKA. Since $CD8^+$ DCs increased preferentially in Flt3L-treated mice, we speculate that these DCs cross-presented and activated malaria-specific $CD8^+$ T cells. These $CD8^+$ T cells were found to produce IFN-γ in response to strain ANKA antigens at levels equal to or even higher than those from untreated mice (Fig. 3B), indicating that priming and IFN-γ production of malaria-specific $CD8^+$ T cells were not impaired in Flt3L-treated mice. However, phenotypic study of the $CD8^+$ T cells in the spleen showed some interesting features. First, we found, unexpectedly, that most $CD8^+$ T cells in *P. berghei* ANKA-infected mice expressed CD11c, an integrin molecule that is often considered a marker of DCs. CD11c expression was also observed on $CD8^+$ T cells after infection with another rodent malaria par-

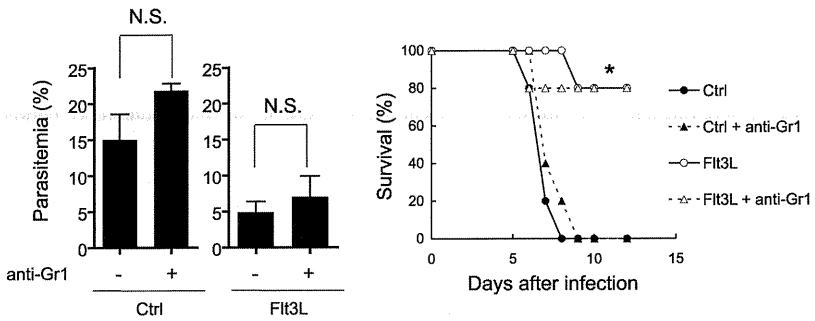

FIG. 6. Role of granulocytes in Flt3L-mediated effects on *P. berghei* ANKA infection. Mice were either left untreated or treated with Flt3L 7 days prior to infection and received an anti-Gr1 MAb (50 μg) i.p. 2 days prior to infection. (Left) The levels of parasitemia 5 days after infection are expressed as means ± SD. N.S., not significant by the Mann-Whitney test. (Right) The survival of infected mice was monitored daily. *, $P < 0.05$ by the log rank test. The experiments were repeated twice, and representative data are shown.

asite, *Plasmodium yoelii* (data not shown), and was previously reported in intraepithelial lymphocytes (IEL) and recently activated $CD8^+$ T cells in virus-infected mice (4, 13, 18). IEL from germ-free mice did not express CD11c, and bacterial colonization induced CD11c in IEL (13). However, antigen-driven activation of $CD8^+$ T cells alone is not sufficient for the induction of CD11c, since we and others failed to induce CD11c on $CD8^+$ T cells through TCR stimulation *in vitro* (data not shown). To our knowledge, this is the first report of CD11c expression in $CD8^+$ T cells during parasite infection. CD11c, which forms a heterodimer with β2 integrin (CD18), is involved in the adhesion of cells via ligands, including ICAM-1, ICAM-2, and VCAM-1 (28). The absence of CD11c significantly attenuated the severity of experimental autoimmune encephalomyelitis and reduced the levels of cellular infiltration and demyelination (5). CD11c may be involved in the activation or effector function of $CD8^+$ T cells during *P. berghei* ANKA infection through its role in strengthening the $CD8^+$ T cell–target cell interaction, thus participating in the pathogenesis of ECM. Alternatively, CD11c may be involved in the preferential accumulation of activated $CD8^+$ T cells in the inflamed brain. However, the expression of CD11c on $CD8^+$ T cells is not sufficient for the onset of ECM, because $CD8^+$ T cells in *P. berghei* ANKA-infected BALB/c mice expressed CD11c at levels similar to those in B6 mice, yet strain ANKA-infected BALB/c mice do not develop ECM (data not shown).

The phenotypic characterization of $CD8^+$ T cells from Flt3L-treated mice during *P. berghei* ANKA infection suggests that their activation status is distinct from that of $CD8^+$ T cells from control mice. We used CD11c as a general activation marker of $CD8^+$ T cells and examined cells that coexpress activation-induced molecules with CD11c. Among $CD11c^+$ $CD8^+$ T cells from *P. berghei* ANKA-infected mice, the expression of CD44 and CXCR3 was similar for Flt3L-treated and untreated mice, while the expression of CD25, CD137, and granzyme B was diminished in Flt3L-treated mice. Conventional DCs play critical roles in the pathogenesis of ECM (10). The differential activation of $CD8^+$ T cells in Flt3L-treated mice may reflect a difference in the type of DCs that were expanded by Flt3L treatment. In support of this possibility, it has been reported that DCs that expanded by *in vivo* administration of Flt3L produced altered cytokine profiles and had tolerogenic effects on T cells (23). DCs are composed of multiple subsets, and the combined action of DC stimulation with Flt3L and *P. berghei* ANKA infection may have resulted in the altered phenotype of the activated $CD8^+$ T cells (27). An alternative possibility is the involvement of other T cells, such as helper or regulatory $CD4^+$ T cells, that were differentially activated in Flt3L-treated mice. However, Flt3L treatment resulted in similarly increased proportions of regulatory $CD4^+$ T cells both with and without *P. berghei* ANKA infection, consistent with the previous report (35). In addition, $CD4^+$ T cells from Flt3L-treated and untreated mice produced similar levels of IFN-γ in response to an anti-TCR MAb. Thus, regulatory $CD4^+$ T cells are unlikely to be involved in the observed phenotypic differences in $CD8^+$ T cells.

Interestingly, the numbers of T cells recovered from the brain were not significantly different for Flt3L-treated versus untreated mice after infection with *P. berghei* ANKA, although Flt3L-treated mice did not develop lethal ECM. CD11c expression in brain-sequestered $CD8^+$ T cells was reduced in Flt3L-treated mice, which might influence the strength of the interaction between $CD8^+$ T cells and their target or local tissue. Functionally, levels of $CD8^+$ T cells that can produce both IFN-γ and granzyme B were significantly reduced in Flt3L-treated mice, supporting the altered activation status of these $CD8^+$ T cells. Finally, the number of pRBC in the brain was dramatically reduced in Flt3L-treated mice, a finding consistent with the lack of ECM in these mice. The results clearly indicate that the accumulation of $CD8^+$ T cells in the brain is not sufficient for the sequestration of pRBC in the brain. We suspect that recruitment of *P. berghei* ANKA-specific activated $CD8^+$ T cells to the brain might condition brain blood vessels for the sequestration of pRBC. In Flt3L-treated mice, $CD8^+$ T cells might not be sufficiently activated to achieve this conditioning, while they themselves were able to be sequestered in the brain.

ECM is a complex process resulting from the intricate interplay of *P. berghei* ANKA infection and the host immune response. We have shown that the development of ECM can be effectively prevented by the administration of Flt3L, which stimulates the innate immune system, including dendritic cells, and indirectly alters the activation status of $CD8^+$ T cells after infection with *P. berghei* ANKA. In addition, the present study indicates that the number of brain-sequestered T cells does not correlate directly with the pathogenesis of ECM. Further detailed analysis of this system may reveal the critical function of the immune system in the pathogenesis of ECM.

ACKNOWLEDGMENTS

We appreciate Y. Yoshikai for providing mice, H. Asao for providing the hybridoma cell line, Y. Yamato and Y. Tsuchiya for technical assistance and secretarial work, M. Masumoto for cell sorting, and R. Kamei for help in animal care. We also thank the members of our laboratory for helpful discussions and advice.

This study was supported by the Global COE Program at Nagasaki University and by Grants-in-Aid from the Ministry of Education, Science, Sports and Culture to K.Y. (21390125).

The authors declare no competing financial interests.

REFERENCES

1. **Baptista, F. G., et al.** 2010. Accumulation of *Plasmodium berghei*-infected red blood cells in the brain is crucial for the development of cerebral malaria in mice. Infect. Immun. **78:**4033–4039.
2. **Belnoue, E., et al.** 2003. CCR5 deficiency decreases susceptibility to experimental cerebral malaria. Blood **101:**4253–4259.
3. **Belnoue, E., et al.** 2002. On the pathogenic role of brain-sequestered αβ $CD8^+$ T cells in experimental cerebral malaria. J. Immunol. **169:**6369–6375.
4. **Beyer, M., et al.** 2005. The β2 integrin CD11c distinguishes a subset of cytotoxic pulmonary T cells with potent antiviral effects *in vitro* and *in vivo*. Respir. Res. **6:**70.
5. **Bullard, D. C., X. Hu, J. E. Adams, T. R. Schoeb, and S. R. Barnum.** 2007. p150/95 (CD11c/CD18) expression is required for the development of experimental autoimmune encephalomyelitis. Am. J. Pathol. **170:**2001–2008.
6. **Campanella, G. S., et al.** 2008. Chemokine receptor CXCR3 and its ligands CXCL9 and CXCL10 are required for the development of murine cerebral malaria. Proc. Natl. Acad. Sci. U. S. A. **105:**4814–4819.
7. **Chen, L., Z. Zhang, and F. Sendo.** 2000. Neutrophils play a critical role in the pathogenesis of experimental cerebral malaria. Clin. Exp. Immunol. **120:**125–133.
8. **den Haan, J. M., S. M. Lehar, and M. J. Bevan.** 2000. $CD8^+$ but not $CD8^-$ dendritic cells cross-prime cytotoxic T cells in vivo. J. Exp. Med. **192:**1685–1696.
9. **de Souza, J. B., J. C. Hafalla, E. M. Riley, and K. N. Couper.** 2009. Cerebral malaria: why experimental murine models are required to understand the pathogenesis of disease. Parasitology **137:**755–772.
10. **deWalick, S., et al.** 2007. Conventional dendritic cells are the critical APC required for the induction of experimental cerebral malaria. J. Immunol. **178:**6033–6037.

11. **Fleming, T. J., M. L. Fleming, and T. R. Malek.** 1993. Selective expression of Ly-6G on myeloid lineage cells in mouse bone marrow. RB6-8C5 mAb to granulocyte-differentiation antigen (Gr-1) detects members of the Ly-6 family. J. Immunol. **151:**2399–2408.
12. **Herweijer, H., and J. A. Wolff.** 2007. Gene therapy progress and prospects: hydrodynamic gene delivery. Gene Ther. **14:**99–107.
13. **Huleatt, J. W., and L. Lefrancois.** 1995. Antigen-driven induction of CD11c on intestinal intraepithelial lymphocytes and $CD8^+$ T cells *in vivo*. J. Immunol. **154:**5684–5693.
14. **Idro, R., N. E. Jenkins, and C. R. Newton.** 2005. Pathogenesis, clinical features, and neurological outcome of cerebral malaria. Lancet Neurol. **4:**827–840.
15. **Ing, R., M. Segura, N. Thawani, M. Tam, and M. M. Stevenson.** 2006. Interaction of mouse dendritic cells and malaria-infected erythrocytes: uptake, maturation, and antigen presentation. J. Immunol. **176:**441–450.
16. **Karsunky, H., M. Merad, A. Cozzio, I. L. Weissman, and M. G. Manz.** 2003. Flt3 ligand regulates dendritic cell development from $Flt3^+$ lymphoid and myeloid-committed progenitors to $Flt3^+$ dendritic cells *in vivo*. J. Exp. Med. **198:**305–313.
17. **Langhorne, J., et al.** 2004. Dendritic cells, pro-inflammatory responses, and antigen presentation in a rodent malaria infection. Immunol. Rev. **201:**35–47.
18. **Lin, Y., T. J. Roberts, V. Sriram, S. Cho, and R. R. Brutkiewicz.** 2003. Myeloid marker expression on antiviral $CD8^+$ T cells following an acute virus infection. Eur. J. Immunol. **33:**2736–2743.
19. **Lundie, R. J., et al.** 2008. Blood-stage *Plasmodium* infection induces $CD8^+$ T lymphocytes to parasite-expressed antigens, largely regulated by $CD8\alpha^+$ dendritic cells. Proc. Natl. Acad. Sci. U. S. A. **105:**14509–14514.
20. **Lundie, R. J., et al.** 2010. Blood-stage *Plasmodium berghei* infection leads to short-lived parasite-associated antigen presentation by dendritic cells. Eur. J. Immunol. **40:**1674–1681.
21. **Maraskovsky, E., et al.** 1996. Dramatic increase in the numbers of functionally mature dendritic cells in Flt3 ligand-treated mice: multiple dendritic cell subpopulations identified. J. Exp. Med. **184:**1953–1962.
22. **McKenna, H. J., et al.** 2000. Mice lacking flt3 ligand have deficient hematopoiesis affecting hematopoietic progenitor cells, dendritic cells, and natural killer cells. Blood **95:**3489–3497.
23. **Miller, G., V. G. Pillarisetty, A. B. Shah, S. Lahrs, and R. P. DeMatteo.** 2003. Murine Flt3 ligand expands distinct dendritic cells with both tolerogenic and immunogenic properties. J. Immunol. **170:**3554–3564.
24. **Miu, J., et al.** 2008. Chemokine gene expression during fatal murine cerebral malaria and protection due to CXCR3 deficiency. J. Immunol. **180:**1217–1230.
25. **Miyakoda, M., et al.** 2008. Malaria-specific and nonspecific activation of $CD8^+$ T cells during blood stage of *Plasmodium berghei* infection. J. Immunol. **181:**1420–1428.
26. **Nitcheu, J., et al.** 2003. Perforin-dependent brain-infiltrating cytotoxic $CD8^+$ T lymphocytes mediate experimental cerebral malaria pathogenesis. J. Immunol. **170:**2221–2228.
27. **Pulendran, B., H. Tang, and S. Manicassamy.** 2010. Programming dendritic cells to induce T_H2 and tolerogenic responses. Nat. Immunol. **11:**647–655.
28. **Sadhu, C., et al.** 2007. CD11c/CD18: novel ligands and a role in delayed-type hypersensitivity. J. Leukoc. Biol. **81:**1395–1403.
29. **Schofield, L., and G. E. Grau.** 2005. Immunological processes in malaria pathogenesis. Nat. Rev. Immunol. **5:**722–735.
30. **Senaldi, G., C. Vesin, R. Chang, G. E. Grau, and P. F. Piguet.** 1994. Role of polymorphonuclear neutrophil leukocytes and their integrin CD11a (LFA-1) in the pathogenesis of severe murine malaria. Infect. Immun. **62:**1144–1149.
31. **Shinkai, Y., et al.** 1992. RAG-2-deficient mice lack mature lymphocytes owing to inability to initiate V(D)J rearrangement. Cell **68:**855–867.
32. **Shortman, K., and S. H. Naik.** 2007. Steady-state and inflammatory dendritic-cell development. Nat. Rev. Immunol. **7:**19–30.
33. **Sponaas, A. M., et al.** 2006. Malaria infection changes the ability of splenic dendritic cell populations to stimulate antigen-specific T cells. J. Exp. Med. **203:**1427–1433.
34. **Sponaas, A. M., et al.** 2009. Migrating monocytes recruited to the spleen play an important role in control of blood stage malaria. Blood **114:**5522–5531.
35. **Swee, L. K., N. Bosco, B. Malissen, R. Ceredig, and A. Rolink.** 2009. Expansion of peripheral naturally occurring T regulatory cells by Fms-like tyrosine kinase 3 ligand treatment. Blood **113:**6277–6287.
36. **Taylor, T. E., et al.** 2004. Differentiating the pathologies of cerebral malaria by postmortem parasite counts. Nat. Med. **10:**143–145.
37. **Van den Steen, P. E., et al.** 2008. CXCR3 determines strain susceptibility to murine cerebral malaria by mediating T lymphocyte migration toward IFN-γ-induced chemokines. Eur. J. Immunol. **38:**1082–1095.
38. **Waskow, C., et al.** 2008. The receptor tyrosine kinase Flt3 is required for dendritic cell development in peripheral lymphoid tissues. Nat. Immunol. **9:**676–683.
39. **Wykes, M. N., et al.** 2007. *Plasmodium* strain determines dendritic cell function essential for survival from malaria. PLoS Pathog. **3:**e96.
40. **Yanez, D. M., D. D. Manning, A. J. Cooley, W. P. Weidanz, and H. C. van der Heyde.** 1996. Participation of lymphocyte subpopulations in the pathogenesis of experimental murine cerebral malaria. J. Immunol. **157:**1620–1624.

Editor: J. F. Urban, Jr.

HUMORAL IMMUNE RESPONSES TO *PLASMODIUM VIVAX* SUBTELOMERIC TRANSMEMBRANE PROTEINS IN THAILAND

Tippawan Sungkapong[1], Richard Culleton[2], Kazuhide Yahata[2], Mayumi Tachibana[3], Ronatrai Ruengveerayuth[4], Rachanee Udomsangpetch[5], Motomi Torii[3], Takafumi Tsuboi[6], Jetsumon Sattabongkot[7], Osamu Kaneko[2,a] and Kesinee Chotivanich[1,a]

[1]Department of Clinical Tropical Medicine, [7]Mahidol Vivax Research Center, Faculty of Tropical Medicine, Mahidol University, Bangkok, Thailand; [2]Department of Protozoology, Institute of Tropical Medicine (NEKKEN) and the Global Center of Excellence Program, Nagasaki University, Sakamoto, Nagasaki, Japan; [3]Department of Molecular Parasitology, Ehime University Graduate School of Medicine, Shitsukawa, Toon, Ehime, Japan; [4]Mae Sot Hospital, Tak, Thailand; [5]Department of Pathobiology, Faculty of Science, Mahidol University, Bangkok, Thailand; [6]Cell-Free Science and Technology Research Center, Ehime University, Matsuyama, Ehime, Japan

Abstract. *Plasmodium vivax* subtelomeric transmembrane protein (PvSTP) is a homolog of *P. falciparum* $SURFIN_{4.2}$, a protein exposed on the parasite-infected erythrocyte (iE) surface, and is thus considered to be exposed on *P. vivax*-iE. Because antibodies targeting antigens located on the surface of *P. falciparum*-iE, such as *P. falciparum* erythrocyte membrane protein 1, play an important role in regulating the course of disease, we evaluated the presence of antibodies in *P. vivax*-infected patients against two PvSTP paralogs, PvSTP1 and PvSTP2. Recombinant proteins corresponding to cysteine-rich domain (CRD) of the PvSTP extracellular region and the cytoplasmic region (CYT) were generated and used for the enzyme-linked immunosorbent assay. Plasma samples (n = 70) reacted positively with recombinant PvSTP1-CRD (40%), PvSTP1-CYT (31%), PvSTP2-CRD (27%), and PvSTP2-CYT (56%), suggesting that PvSTP1 and -2 are naturally immunogenic. Specific response against either PvSTP1 or PvSTP2 indicates the existence of specific antibodies for either PvSTP1 or -2.

Keywords: *P. vivax*, PvSTP, ELISA, antibody response

INTRODUCTION

Plasmodium vivax accounts for more than 50% of all malaria cases outside of Africa. The parasite causes extensive morbidity in endemic countries, and its socio-economic impact, although large, is somewhat neglected (Mueller *et al*, 2009). However, there is mounting evidence that *P. vivax* can lead to severe malaria associated with, for example, pulmonary edema, anemia, and sometimes death (Kochar *et al*, 2005; Kumar *et al*, 2007). One of the factors associated with the

Correspondence: Kesinee Chotivanich, Department of Clinical Tropical Medicine, Faculty of Tropical Medicine, Mahidol University, 420/6 Ratchawithi Road, Ratchathewi, Bangkok 10400, Thailand.
Tel/Fax: 66 (0) 2644 4541/66 (0) 2644 4541
E-mail: nok@tropmedres.ac
[a]These authors contributed equally to this work

severity of falciparum malaria is rosette formation, which is defined as two or more uninfected erythrocytes adhering to a parasite-infected erythrocyte (iE) (David *et al*, 1988; Handunnetti *et al*, 1989; Carlson *et al*, 1990; Kaul *et al*, 1991). Rosette formation is also seen in *P. vivax*, predominantly at the trophozoite and schizont stages (Udomsanpetch *et al*, 1995; Chotivanich *et al*, 1998). This phenomenon is also seen in other malaria spp, including the human malaria parasites *P. ovale* and *P. malariae* (Lowe *et al*, 1998), the primate malaria parasites *P. fragile* and *P. coatneyi*, and the rodent malaria parasite, *P. chabaudi* (Udomsangpetch *et al*, 1991; Mackinnon *et al*, 2002). In *P. falciparum*, the major ligand involved in rosette formation is believed to be *P. falciparum*-erythrocyte membrane protein 1 (PfEMP1), which is located on the surface of the parasite-iE; however, homologs of PfEMP1 are not found in *P. vivax* (Rowe *et al*, 1997).

In *P. falciparum*, a protein termed *Pf*SURFIN$_{4.2}$ is expressed on both the surface of the merozoite and the iE (Winter *et al*, 2005). *Pf*SURFIN$_{4.2}$ is a type I transmembrane protein, encoded by one of the members of the surface-associated interspersed (*surf*) multigene family. *P. vivax* possesses a SURFIN ortholog, termed *P. vivax* subtelomeric transmembrane protein 1 (PvSTP1) (del Portillo *et al*, 2001). The N-terminal extracellular regions of both *Pf*SURFIN$_{4.2}$ and PvSTP1 are composed of a moderately conserved cysteine-rich domain (CRD) and a variable region (VAR), and the C-terminal cytoplasmic region (CYT) is composed of semi-conserved triple or single tryptophan-rich domains (WR), respectively (Winter *et al*, 2005). PvSTP1 has at least one paralog in the *P. vivax* genome, which we termed as PvSTP2 (PVX_090285) and collectively we called them PvSTP, hereafter. The extracellular region of PvSTP has homology with the members encoded by *P. vivax* interspersed repeat (*vir*) multigene family, which consists of around 350 members, some of which have been shown to be located on the parasite-iE surface (del Portillo *et al*, 2001). The orthologs of *vir* also are found in primate and rodent malaria parasites and are collectively termed *Plasmodium* interspersed repeat (*pir*) multigene family. The homology between PvSTP extracellular region and *pir* gene products is likely a result of gene expansion of the former to create the latter. Even if this is the case, the fact that PvSTP genes are still retained by the parasite suggests that they are still functional and may play important roles on the parasite-iE, such as in rosette formation or cytoadhesion.

The development of a vaccine against *P. vivax* is urgent. Efforts have focused on, for example, molecules expressed on the merozoite surface (apical membrane antigen-1, AMA1; merozoite surface protein 1, MSP1; and Duffy binding protein, DBP), on sporozoite surface (circumsporozoite protein, CSP), and on oocyst/ookinete surface (Pvs25) (Arévalo-Herrera *et al*, 2010). However, studies of the molecules expressed on *P. vivax*-iE have been limited: only one study was conducted for VIR, a protein product of *vir*, in northern Brazil (Oliveira *et al*, 2006). It is important to evaluate the natural immune response among individuals in vivax malaria endemic areas, to identify potential vaccine target antigens. Therefore, we evaluated the naturally acquired antibody responses against PvSTP1 and -2, using plasma obtained from *P. vivax*-infected patients in the western border of Thailand.

Table 1
Characteristics of the study population.

	Age (years)	Body temperature (°C)	Parasite density (parasites/μl)	Hemoglobin concentration (g/dl)
Median	22	37	8,000	13.8
Range	(13-45)	(35-40)	(40-44,000)	(10.9-17)
Number	24	23	70	22

MATERIALS AND METHODS

Study site and sample collection

Seventy patients, who visited the outpatient clinic of Mae Sot Hospital, Tak Province, Thailand, and were positive for *P. vivax* by microscopic examination of blood smears, were recruited for this study. Patients were treated with chloroquine (2,500 mg) for 3 days and primaquine (15 mg) for 14 days (15 mg of primaquine was given for 8 times in patients with G6PD deficiency). Informed consent was obtained from all adult participants and from parents or legal guardians of minors. Subsequent to obtaining informed consent, 10 ml of blood was drawn into a heparinized tube and centrifuged at 800*g* for 5 minutes and plasma was collected. Parasite density was determined (Shute, 1988) and *P. vivax* infection was reconfirmed by polymerase chain reaction (PCR)-based diagnosis (Snounou, 1996). Plasma were also collected from 11 volunteers in Thailand who had no history of malaria infection and used as negative control. Only 24 patients allowed collection of the clinical history (age, body temperature, hemoglobin concentration, and past history of malaria infection) by interview and medical records (Table 1). This study was approved by Ethical Review Committee of Mahidol University, No. MUTM.2006-020.

Recombinant protein preparation

The recombinant proteins were produced as described previously (Tsuboi *et al*, 2008). In brief, a DNA linker (5'-AGATATCCCCGGGAGGCCTAAGCT-3' and 5'-TAGGCCTCCCGGGGATATCTAGCT-3') containing *Eco*RV, *Sma*I and *Stu*I sites was inserted into the *Sac*I site of pEU-E01-HisGST(TEV)-N2, an expression plasmid encoding N-terminal hexa-His-tag and glutathione S transferase (GST)-tag followed by a tobacco etch virus (TEV) protease cleavage site, designed specifically for a wheat germ cell-free protein expression system (CellFree Sciences, Matsuyama, Japan), to yield pEU-HGtevK_ES. A DNA fragment corresponding to nucleotide positions (nt) 4 - 642 of the PvSTP1 gene was PCR-amplified from genomic (g)DNA of *P. vivax* (isolated from a Japanese patient who visited Myanmar in 2005) and ligated into the *Eco*RV site of pEU-HGtevK_ES, to produce a plasmid expressing recombinant protein consisting of 6xHis-GST followed by the N-terminal CRD of PvSTP1 (H-GST-vSTP1-CRD). In a similar manner, DNA fragments corresponding to nt 1608 - 2675 of PvSTP1 (encoding putative cytoplasmic region, CYT), nt 4 - 645 of PvSTP2 (CRD), and nt 1932 - 3203 of PvSTP2 (CYT) were PCR-amplified from gDNA of *P. vivax* Salvador I strain (Sal-I), and were subsequently ligated into *Eco*RV site of pEU-HGtevK_ES,

Table 2
Oligonucleotide used for recombinant protein production.

Protein	Region	Sequence[a]
PvSTP1	CRD	gggTCATTTCAAAATCAATTTAAATTAG
		gggTCGAATATGTGCTGGAATATG
	CYT	gggACCATTATAGATATACACTTGG
		gggCTAAATTACATTAATGTTTTGCTT
PvSTP2	CRD	gggGCATACGCAAAAATAATTAATTTTG
		gggCAAACTATAGGGAAGATGATG
	CYT	gggGGCTCAAAAACGATTGTAGAG
		gggTTACCCGTTGTATGTTGCATAA

[a]Triple guanine (g) residues were added to the 5′ end of each primer to prevent deletions of the 5′ and 3′ end of the PCR products during the ligation step, in which both EcoRV enzyme and T4 DNA ligase were present at the same time in the tube (Ghoneim *et al*, 2007).

to express the recombinant proteins, H-GST-vSTP1-CYT, H-GST-vSTP2-CRD, and H-GST-vSTP2-CYT, respectively (nt positions are based on Sal-I gDNA sequence). Oligonucleotides, based upon Sal-I sequence, used in the PCR amplification are summarized in Table 2. Recombinant His-GST-fused proteins were absorbed onto a glutathione-Sepharose 4B column, subjected to the TEV protease cleavage to remove N-terminal His-GST region, and eluted with phosphate buffered saline (PBS) to obtain recombinant (r) proteins rPvSTP1-CRD, rPvSTP1-CYT, rPvSTP2-CRD, and rPvSTP2-CYT, respectively (Figs 1 and 2). As a negative control, recombinant His-GST (rGST) was expressed from pEU-HG(tev)N02.

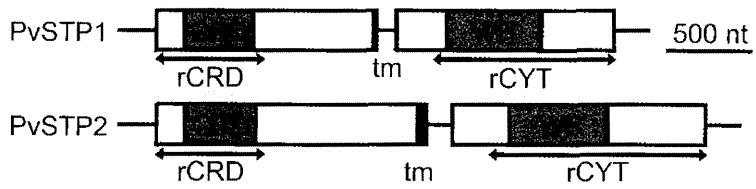

Fig 1–Schematic representation of the exon-intron regions for the genes encoding for PvSTP1 and -2 and domains of the encoded proteins. CRD, tm, and WR indicates cysteine-rich domain, transmembrane region, and tryptophan-rich domain, respectively. Regions used to generate recombinant proteins are indicated by lines with arrow under each scheme. rCRD and rCYT indicates recombinant proteins for CRD and putative cytoplasmic region, respectively.

Enzyme-linked immunosorbent assay (ELISA)

Flat-bottom 96-well microtiter plates (Sumitomo Bakelite, Tokyo, Japan) were coated with 50 µl of 1 µg/ml each recombinant protein in carbonate buffer (pH 9.6) and incubated overnight at 4°C. After washing with PBS containing 0.05% Tween 20 (PBS-T), each well was blocked with 200 µl of blocking buffer (PBS containing 0.05% Tween 20 and 5% skim milk) for 30 minutes at 37°C. Fifty microliter aliquots of plasma-containing blocking buffer (1:50 dilution) were added into each well, each plasma sample in triplicate at a single plate, and incubated for 2 hours at 37°C.

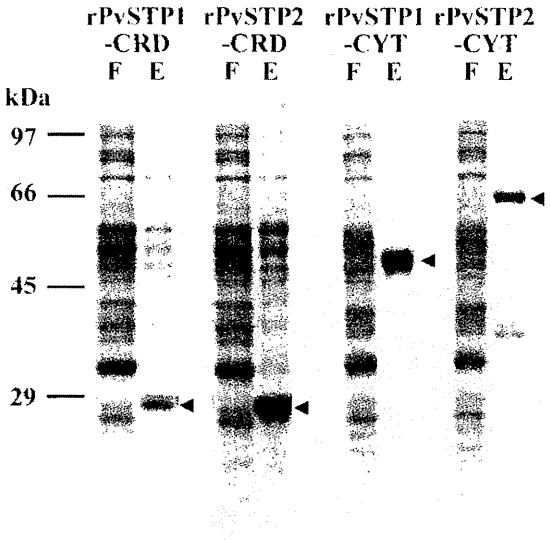

Fig 2–SDS-PAGE analysis of the recombinant PvSTP1 and PvSTP2 proteins. Recombinant proteins were separated on SDS-12.5% polyacrylamide gel-electrophoresis under reducing condition and stained with Coomassie brilliant blue. F and E indicates flow through of the GST-affinity column containing unbound proteins and eluate from the column after TEV protease cleavage, respectively (Tsuboi *et al*, 2008). Arrowheads indicate purified recombinant proteins; CRD, cysteine-rich domain; CYT, cytoplasmic region.

After washing with PBS-T, 50 µl aliquots of horseradish peroxide-conjugated goat anti-human IgG (H+L; 1:10,000 dilution; Promega, Madison, WI) were added into each well and the plates were incubated for 1.5 hours at room temperature. After further washing, 50 µl aliquots of ABTS [2,2 2-Azino-bis (3-ethylabenzothiazoline-6-sulfonic acid) diammonium salt; Sigma, St Louis, MO] were added into each well and the plates were incubated for 30 minutes at 37°C. The reaction was terminated by the addition of 50 µl/well of 1 M NaF solution (Wako, Osaka, Japan), and absorbance measured using an automated microplate reader (iMark™; Bio-Rad, Hercules, CA) at 405 nm.

Data analysis

The adjusted absorbance value of each sample was obtained by dividing the mean optical density (OD) value of each individual sample by the mean OD value for the 11 malaria non-exposed individuals (baseline). Samples with adjusted absorbance values greater than the baseline absorbance +5 standard deviation (SD) were considered to be positive for antibodies to the antigen tested. Statistical analyses were performed using PASW Statistics 18 software version 11.5 (SPSS, New York, NY). The differences of adjusted absorbance values to each antigen between vivax patients and malaria non-exposed people were assessed by Mann-Whitney *U* test. The correlations between responses to each antigen were analyzed by Spearman's rank test. The correlations of parasite density with adjusted absorbance value to each antigen were analyzed by Spearman's rank test. *P*-values ≤ 0.05 are considered statistically significant.

RESULTS

Antibody responses to rPvSTP1 and -2

The antibody responses against rPvSTP were determined by ELISA for 70 samples collected from *P. vivax*-infected patients. The comparative antibody responses to PvSTP1 and -2 between *P. vivax* patients and malaria non-exposed controls to each PvSTP region were significantly different ($p < 0.01$, Mann-Whitney *U* test) (Fig 3). The percentage of plasma that recognized any of the rPvSTP1 and -2 proteins was 54% (38/70) and 64% (45/70), respectively. The percent positive rates were 40% for rPvSTP1-CRD (28/70), 31% for rPvSTP1-CYT (22/70), 27% for rPvSTP2-CRD (19/70), and 56% for rPvSTP2-CYT (39/70) (Fig 4). All plasma

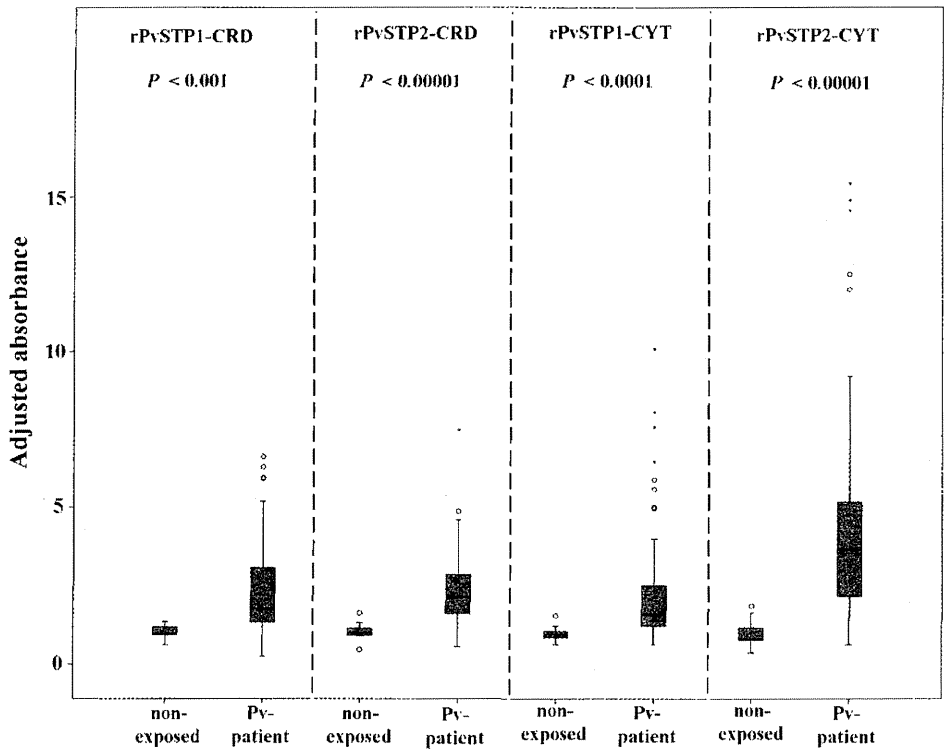

Fig 3–Antibody responses against rPvSTP1 and -2 of *P. vivax*-infected patients' plasma. Values represent adjusted absorbance for each antigen (rPvSTP1-CRD, rPvSTP2-CRD, rPvSTP1-CYT, and rPvSTP2-CYT). Box plots represent median values with 25th and 75th percentiles. Each bar marks the 10th and 90th percentiles. Outlier and extreme values are plotted as stars and circles, respectively. CRD and CYT indicates the cysteine-rich domain and cytoplasmic region, respectively. Differences are assessed by Mann-Whitney *U* test.

samples were negative for rGST (data not shown). Of the patients' plasma, 17% (12/70) and 19% (13/70) reacted positively to both CRD and CYT regions of PvSTP1 and -2, respectively. The adjusted absorbance values against each recombinant PvSTP proteins are shown in Fig 4.

Significant correlations of adjusted absorbance values were observed between anti-PvSTP1 and -2 in each antigen region (CRD: $R = 0.74$, $p < 0.01$; CYT: $R = 0.48$, $p < 0.01$) using Spearman's rank test, suggesting cross-reactivity between anti-PvSTP1 and -2, or a co-exposure of both proteins to host immunity. No significant correlation was found between antibody response to rPvSTP and parasite density.

Specific antibody response to PvSTP1 and -2 in *P. vivax*-infected patients

To evaluate the degree of cross-reactivity between anti-PvSTP1 and -2, ELISA positive samples were grouped for each antigen region, according to their reactivity against PvSTP1 or -2 (Fig 5). Some patients were positive only for either PvSTP1 or -2, indicating the existence of specific antibodies for either PvSTP1 or -2. More samples were positive only for rPvSTP1-CRD (12 cases) than the samples only positive for rPvSTP2-CRD (3 cases),

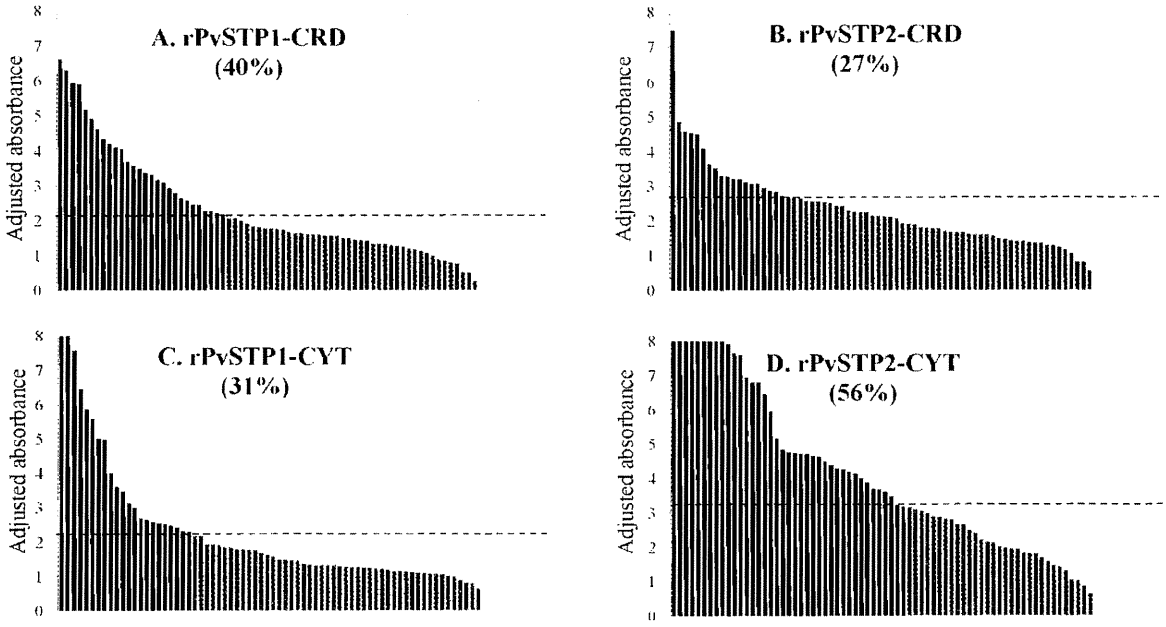

Fig 4–Individual antibody responses to recombinant proteins for PvSTP1 and PvSTP2. (A) rPvSTP1-CRD, (B) rPvSTP2-CRD, (C) rPvSTP1-CYT, and (D) rPvSTP2-CYT. Antibody responses against recombinant proteins are expressed as adjusted absorbance values for *P. vivax*-infected patient plasma in black and gray (n = 70) and for malaria non-exposed individuals (n = 11) as white. Dashed lines indicate positive cut-off values for each antigen, obtained by calculation of mean value + 5 standard deviation of adjusted absorbance values from the 11 malaria non-exposed individuals in Thailand. Positive rates are shown in parentheses. CRD and CYT, indicates the cysteine-rich domain and cytoplasmic region, respectively.

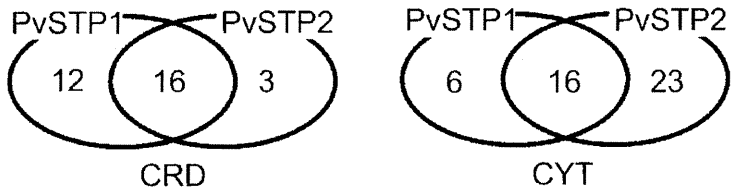

Fig 5–Specific response to rPvSTP1 and -2 in *P. vivax*-infected patients. Numbers indicate individuals positive for antibodies specific to rPvSTP1 or rPvSTP2. CRD and CYT indicates the cysteine-rich domain and cytoplasmic region, respectively.

suggesting that the extracellular region of PvSTP1 was more immunogenic than PvSTP2, or patients were exposed to the extracellular region of PvSTP1 more frequently than to that of PvSTP2. On the other hand, more samples were positive only for rPvSTP2-CYT (23 cases) than positive only for rPvSTP1-CYT (6 cases), suggesting the PvSTP2 cytoplasmic region was more immunogenic than that of

PvSTP1, or that the PvSTP2 cytoplasmic region was more frequently exposed to the patient's immune system than the PvSTP1 cytoplasmic region.

DISCUSSION

This is the first report showing evidence that PvSTP1 and -2 are immunogenic in natural infection. Our results suggest that both PvSTP1 and -2 elicit specific antibodies. Proteins on the surface of malaria iEs have been a major focus of malaria research because of their role in pathogenesis and their potential as targets for immunity and for vaccine development. In *P. vivax*, however, only VIR family proteins have been studied (del Portillo *et al*, 2001). In a malaria-endemic area in Brazil, 49.0% of vivax malaria patients possessed antibodies (IgG or IgM) against at least one of 4 distinct types of VIR protein; however, IgG response against each VIR type proteins was lower (2.0 - 17.5%) (Oliveira *et al*, 2006). In the same study, the positive rate of IgG antibodies against two *P. vivax* merozoite proteins, PvAMA1 and PvMSP1-19kD region, were found to be 57% and 90.5%, respectively. Thus, it was concluded that the prevalence of antibodies against each VIR was much lower than those against PvAMA1 and PvMSP1-19kDa. In this study, we evaluated antibody responses (IgG or IgM) against PvSTP1 and -2 in plasma of *P. vivax*-infected patients living in endemic area of Thailand and found that 44% of patients produced antibodies against the extracellular region of rPvSTP1 or -2 (40% for rPvSTP1 and 27% for rPvSTP2) a percentage similar to that previously recorded for the VIR family proteins (Oliveira *et al*, 2006).

Initially, we expected that the extracellular CRD region, would be more immunogenic than the cytoplasmic CYT region, but our results showed that this was not the case for PvSTP2, in which the CYT region was more immunogenic than the CRD region. A possible explanation is that the recombinant PvSTP2 cytoplasmic region used in this study may contain epitope(s) that induce high levels of antibody production.

In summary, the presence of antibodies in Thai *P. vivax*-infected patients to recombinant proteins corresponding to *P. vivax* subtelomeric transmembrane protein indicate that PvSTP1 and -2 are naturally immunogenic. The characteristics of these proteins need to be further investigated.

ACKNOWLEDGEMENTS

We thank Kana Kato for technical assistance. This work was supported in part by Grants-in-Aids for Scientific Research 20406009 (to OK), 21249028 (to TT) and the Global COE Program, Nagasaki University, from the Ministry of Education, Culture, Sports, Science and Technology of Japan (to OK), and a Japanese Ministry of Education, Culture, Sports, Science and Technology Special Coordination Fund for Promoting Science and Technology Tenure-Track Research Support Grant (to RC). Funding was provided also by the Commission on Higher Education Staff Development Project, Naresuan University, Thailand; Thailand Research Fund through the Royal Golden Jubilee PhD program; The German Academic Exchange Service (DAAD) and the Faculty of Tropical Medicine, Mahidol University (to TS), and the Thailand Research Fund through the Royal Golden Jubilee PhD program, Faculty of Tropical Medicine, Mahidol University (to KC).

REFERENCES

Arévalo-Herrera M, Chitnis C, Herrera S. Current status of *Plasmodium vivax* vaccine. *Hum Vaccin* 2010; 6: 124-32.

Carlson J, Helmby H, Wahlgren M, *et al.* Human cerebral malaria: association with erythrocyte rosetting and lack of anti-rosetting antibodies. *Lancet* 1990; 336: 1457-60.

Chotivanich KT, Pukrittayakamee S, Simpson JA, White NJ, Udomsangpetch R. Characteristics of *Plasmodium vivax*-infected erythrocyte rosettes. *Am J Trop Med Hyg* 1998; 59: 73-6.

David PH, Handunnetti SM, Leech JH, Gamage P, Mendis KN. Rosetting: a new cytoadherence property of malaria-infected erythrocytes. *Am J Trop Med Hyg* 1988; 38: 289-97.

del Portillo HA, Fernandez-Becerra C, Bowman S, *et al.* A superfamily of variant genes encoded in the subtelomeric region of *Plasmodium vivax*. *Nature* 2001; 410: 839-42.

Ghoneim A, Kaneko O, Tsuboi T, Torii M. The *Plasmodium falciparum* RhopH2 promoter and first 24 amino acids are sufficient to target proteins to the rhoptries. *Parasitol Int* 2007; 56: 31-43.

Handunnetti SM, David PH, Perera KL, Mendis KN. Uninfected erythrocytes form "rosettes" around *Plasmodium falciparum* infected erythrocytes. *Am J Trop Med Hyg* 1989; 40: 115-8.

Kaul DK, Roth EF Jr, Nagel RL, Howard RJ, Handunnetti SM. Rosetting of *Plasmodium falciparum*-infected red blood cells with uninfected red blood cells enhances microvascular obstruction under flow conditions. *Blood* 1991; 78: 812-9.

Kochar DK, Saxena V, Singh N, Kochar SK, Kumar SV, Das A. *Plasmodium vivax* malaria. *Emerg Infect Dis* 2005; 11: 132-4.

Kumar S, Melzer M, Dodds P, Watson J, Ord R. *P. vivax* malaria complicated by shock and ARDS. *Scand J Infect Dis* 2007; 39: 255-6.

Lowe BS, Mosobo M, Bull PC. All four species of human malaria parasites form rosettes. *Trans R Soc Trop Med Hyg* 1998; 92: 526.

Mackinnon MJ, Walker PR, Rowe JA. *Plasmodium chabaudi*: rosetting in a rodent malaria model. *Exp Parasitol* 2002; 101: 121-8.

Mueller I, Galinski MR, Baird JK, *et al.* Key gaps in the knowledge of *Plasmodium vivax*, a neglected human malaria parasite. *Lancet Infect Dis* 2009; 9: 555-66.

Oliveira TR, Fernandez-Becerra C, Jimenez MC, Del Portillo HA, Soares IS. Evaluation of the acquired immune responses to *Plasmodium vivax* VIR variant antigens in individuals living in malaria-endemic areas of Brazil. *Malar J* 2006; 5: 83.

Rowe JA, Moulds JM, Newbold CI, Miller LH. *P. falciparum* Rosetting mediated by a parasite-variant erythrocyte membrane protein and complement-receptor 1. *Nature* 1997; 388: 292-5.

Shute GT. The microscopic diagnosis of malaria. In: Wernsdorfer WH, McGregor I, eds. Malaria: principles and practice of malariology. New York: Churchill Livingstone, 1988: 781-814.

Snounou G. Detection and identification of the four malaria parasite species infecting humans by PCR amplification. *Methods Mol Biol* 1996; 50: 263-91.

Tsuboi T, Takeo S, Iriko H, *et al.* Wheat germ cell-free system-based production of malaria proteins for discovery of novel vaccine candidates. *Infect Immun* 2008; 76: 1702-8.

Udomsangpetch R, Brown AE, Smith CD, Webster HK. Rosette formation by *Plasmodium coatneyi*-infected red blood cells. *Am J Trop Med Hyg* 1991; 44: 399-401.

Udomsanpetch R, Thanikkul K, Pukrittayakamee S, White NJ. Rosette formation by *Plasmodium vivax*. *Trans R Soc Trop Med Hyg* 1995; 89: 635-7.

Winter G, Kawai S, Haeggstrom M, *et al.* SURFIN is a polymorphic antigen expressed on *Plasmodium falciparum* merozoites and infected erythrocytes. *J Exp Med* 2005; 201: 1853-63.

OPEN ACCESS Freely available online

PLoS one

Plasmodium falciparum: Differential Selection of Drug Resistance Alleles in Contiguous Urban and Peri-Urban Areas of Brazzaville, Republic of Congo

Yoko Tsumori[1], Mathieu Ndounga[2], Toshihiko Sunahara[3], Nozomi Hayashida[1], Megumi Inoue[1], Shusuke Nakazawa[1], Prisca Casimiro[2], Rie Isozumi[1], Haruki Uemura[1], Kazuyuki Tanabe[4], Osamu Kaneko[1], Richard Culleton[1,4,5]*

1 Department of Protozoology, Institute of Tropical Medicine (NEKKEN), and the Global COE Program, Nagasaki University, Nagasaki, Japan, **2** Centre d'Etudes des Resources Vegetales, Brazzaville, Republic of Congo, **3** Department of International Health, Institute of Tropical Medicine (NEKKEN), Nagasaki University, Nagasaki, Japan, **4** Laboratory of Malariology, International Research Centre of Infectious Diseases, Research Institute of Microbial Diseases, Osaka University, Osaka, Japan, **5** Malaria Unit, Institute of Tropical Medicine (NEKKEN), Nagasaki University, Nagasaki, Japan

Abstract

The African continent is currently experiencing rapid population growth, with rising urbanization increasing the percentage of the population living in large towns and cities. We studied the impact of the degree of urbanization on the population genetics of *Plasmodium falciparum* in urban and peri-urban areas in and around the city of Brazzaville, Republic of Congo. This field setting, which incorporates local health centers situated in areas of varying urbanization, is of interest as it allows the characterization of malaria parasites from areas where the human, parasite, and mosquito populations are shared, but where differences in the degree of urbanization (leading to dramatic differences in transmission intensity) cause the pattern of malaria transmission to differ greatly. We have investigated how these differences in transmission intensity affect parasite genetic diversity, including the amount of genetic polymorphism in each area, the degree of linkage disequilibrium within the populations, and the prevalence and frequency of drug resistance markers. To determine parasite population structure, heterozygosity and linkage disequilibrium, we typed eight microsatellite markers and performed haplotype analysis of the *msp1* gene by PCR. Mutations known to be associated with resistance to the antimalarial drugs chloroquine and pyrimethamine were determined by sequencing the relevant portions of the *crt* and *dhfr* genes, respectively. We found that parasite genetic diversity was comparable between the two sites, with high levels of polymorphism being maintained in both areas despite dramatic differences in transmission intensity. Crucially, we found that the frequencies of genetic markers of drug resistance against pyrimethamine and chloroquine differed significantly between the sites, indicative of differing selection pressures in the two areas.

Citation: Tsumori Y, Ndounga M, Sunahara T, Hayashida N, Inoue M, et al. (2011) *Plasmodium falciparum*: Differential Selection of Drug Resistance Alleles in Contiguous Urban and Peri-Urban Areas of Brazzaville, Republic of Congo. PLoS ONE 6(8): e23430. doi:10.1371/journal.pone.0023430

Editor: Georges Snounou, Université Pierre et Marie Curie, France

Received May 4, 2011; **Accepted** July 16, 2011; **Published** August 15, 2011

Funding: This work was supported by a Japanese Ministry of Education, Culture, Sports, Science and Technology (MEXT)'s Special Coordination Funds for Promoting Science and Technology Tenure-Track Research Grant (to R.C.), and a Grant-in-Aid for Scientific Research from the Japan Society for the Promotion of Science No. 17–05495 (to R.C. and K.T.). The funders had no role in study design, data collection and analysis, decision to publish, or preparation of the manuscript.

Competing Interests: The authors have declared that no competing interests exist.

* E-mail: richard@nagasaki-u.ac.jp

Introduction

Africa's population is expected to triple by 2050, when it is estimated that 800 million people (half the population) will reside in urban areas [1], with the most significant urbanization occurring in West Africa, where 66% of the population will live in urban areas in 10–15 years time [2]. In 2004, the Pretoria Statement on Urban Malaria was issued. It declares that "Urban malaria in sub-Saharan Africa is a major health problem and is likely to increase in importance unless addressed" [2]. Currently, relatively little is known about the consequences of urbanization for malaria epidemiology, even though it is likely to become significantly more important in the coming years. Certainly, it is likely that transmission rates and parasite prevalences in urban areas are lower than in peri-urban and rural areas, due, for the most part, to lower entomological inoculation rates associated with reduced vectorial capacities [3,4]. However, the consequences of this reduced transmission for parasite genetic diversity, the acquisition of host immunity and the selection and spread of parasite drug resistance remain unclear. Previous studies comparing these factors between areas of varying transmission intensities have usually done so using data from non-contiguous areas. In reality, the process of urbanization in sub-Saharan Africa creates islands of low transmission areas surrounded by regions of higher transmission, so that in order to understand how the expansion of urban centres into the surrounding peri-urban regions will impact on malaria transmission and epidemiology, it is important to compare parasite populations in contiguous peri-urban and urban areas.

The relationship between transmission rates and parasite genetic diversity is important, as the rate of acquisition of

immunity against a parasite population depends to some degree on both these factors. It has been shown, for example, that immunity to malaria is strain-specific [5,6,7,8], and that increased transmission leads to an increase in the number of strains in circulation within a population [9,10,11]. There are a limited number of reports that describe the relationships between transmission rates and parasite genetic diversity, and these have produced conflicting conclusions. Analyses conducted in Senegal [12], Tanzania and Sudan [13] and Papau New Guinea and Tanzania [14] demonstrate significantly lower multiplicities of infection (MOI) and parasite population genetic diversity in low transmission areas compared to high transmission areas. Conversely, studies conducted in Tanzania [15], West Uganda [16], Burkina Faso [17] and Papua New Guinea [18] report no correlation between transmission intensity and MOI and parasite genetic diversity. In all these cases, the high and low transmission areas were non-contiguously located, often separated by hundreds of kilometres, and in two cases were situated in different countries. In this study, we investigate the degree of parasite genetic diversity and MOI from contiguous areas of high and low transmission.

How urbanization will affect the selection and spread of drug resistance is currently very poorly understood. However, the relationships between transmission intensity and drug resistance has been the subject of theoretical modelling and some field studies, again, with conflicting results. Theoretical models predominantly propose three main potential ways that transmission intensity can influence the spread of drug resistance; i) resistance is predominantly selected when transmission intensity is high [19], ii) resistance is predominantly selected when transmission intensity is low [20,21,22], or resistance is predominantly selected at high and low transmission intensities, with less selective pressure at intermediate levels [23,24,25]. The relationships between transmission intensity and drug resistance selection pressure are complex, and involve many factors including within-host competition between parasites [24], fitness costs of drug resistance [26], the consequences of host immunity [27], levels of community drug use [28], and parasite recombination rates [24,29,30]. Empirical data that support these models is scarce. The way in which chloroquine (CQ) and sulphadoxine/pyrimethamine (SP) resistance first arose in areas of low transmission intensity before spreading world-wide [31,32,33], suggests that low transmission intensity conditions may be optimal for the selection of drug resistance, at least *de novo*. In Uganda, Talisuna *et al* (2007) describe a situation in which the highest levels of resistance to both CQ and SP, as measured by treatment failure and the prevalences of molecular markers of resistance, were always higher in the highest transmission areas. For CQ, resistance was also high at the lowest transmission rates, and was at its lowest in areas of intermediate transmission intensity. This was not the case for SP resistance, for which levels of resistance were proportional to transmission intensities [34].

Here, we investigate the relationships between transmission intensity, parasite genetic diversity and the selection of drug resistance in contiguous urban and peri-urban regions of Brazzaville, Republic of Congo, in an attempt to better understand the role of urbanization on malaria epidemiology.

Materials and Methods

Sample collection

A total of 356 blood samples were collected from all patients visiting two health centers within the city of Brazzaville, Republic of Congo between mid August and mid November 2005 corresponding to the beginning of the wet season. There were no age restrictions, and all patients were sampled, regardless of their symptoms. Blood (~50 µl) was applied to Whatman® FTA® Classic Filter Paper cards (Whatman®, USA) *via* finger prick, and left to air-dry. Thick blood smears were also prepared for each sample, stained with Giemsa's solution, and examined on-site by an experienced microscopist. All patients provided data on their age, sex, clinical symptoms before presentation at the health center, region of habitation (whether urban or peri-urban), and which type (if any) anti-malarial drug treatment had been used prior to presentation. Patients were number coded to preserve anonymity. A further 150 samples were collected from a health centre near Pointe-Noire, a city on the west coast of the country, approximately 380 km from Brazzaville, and 141 from a health centre near Gamboma, a town approximately 250 km to the North of Brazzaville, in 2006. These samples were collected on Whatman® 31ETCHR filter paper. RI. Blood spots on filter paper were shipped to Japan in November 2005 (Brazzaville) or November 2006 (Pointe-Noire and Gamboma), stored in individual plastic bags kept at 4°C and DNA was extracted within 2 months of their arrival. Ethics approval for these collections was obtained from the Osaka University Committee for Ethics in Scientific Research, Osaka University, Osaka, Japan, and sampling was authorized by the administrative authority of the Ministry for Research and Ministry for Health in the Republic of Congo. Written informed consent was obtained from individual patients (or their legal guardians), and anti-malarial treatment was provided when appropriate

Study site, population, and classification of urban and peri-urban districts

Brazzaville, the capital of the Republic of Congo, has a population of about 1,000,000. It has a humid tropical climate with two seasons; the rainy season, which begins in September and lasts until May, is characterized by abundant rainfall and violent evening storms. During the dry season, which begins in June and ends in September, there is practically no rain at all [35]. The main malaria vector is *Anopheles gambiae*. The two health centers from which samples were collected for this study (Tenrikyo and Madibou) are located 8 km apart within the southern district of Brazzaville (Figure 1). Tenrikyo health center is situated within the urban region of the district of Makélékélé, and provides health services for patients from the urban regions (*i.e.* areas with a population of more than 1000 persons per km^2, as defined by Hay *et al* (2005)[36] of Makélékélé, Bacongo and Mfilo. Occasionally, patients form the peri-urban area of Makélékélé (Poto-Poto Djoué) also present here. Madibou health center is situated in the peri-urban region of Makélékélé, and serves patients exclusively from peri-urban areas (*i.e.* areas with populations of between 250 and 1000 persons per km^2, as defined by Hay *et al*, 2005) Patients from both health centers were asked to identify the districts in which they lived, and were assigned to either the "urban" or the "peri-urban" group. Two hundred and two blood samples were collected from Madibou health center, and 154 from Tenrikyo.

The urban and peri-urban districts from which patients were recruited are in very close proximity to each other, in places separated by only a few hundred meters, and the parasitological, epidemiological and entomological differences between them were previously described in detail by Trape *et al* (1987) [35,37, 38,39,40]. The urban areas are characterized by low malaria transmission rates (2–12 infective mosquito bites per person per year [37]) and meso-endemicity (parasite prevalences of ~39%, as determined by active case detection of school children within Bacongo in 1984 [37], and the peri-urban areas by high transmission rates (~50 infective mosquito bites per person per

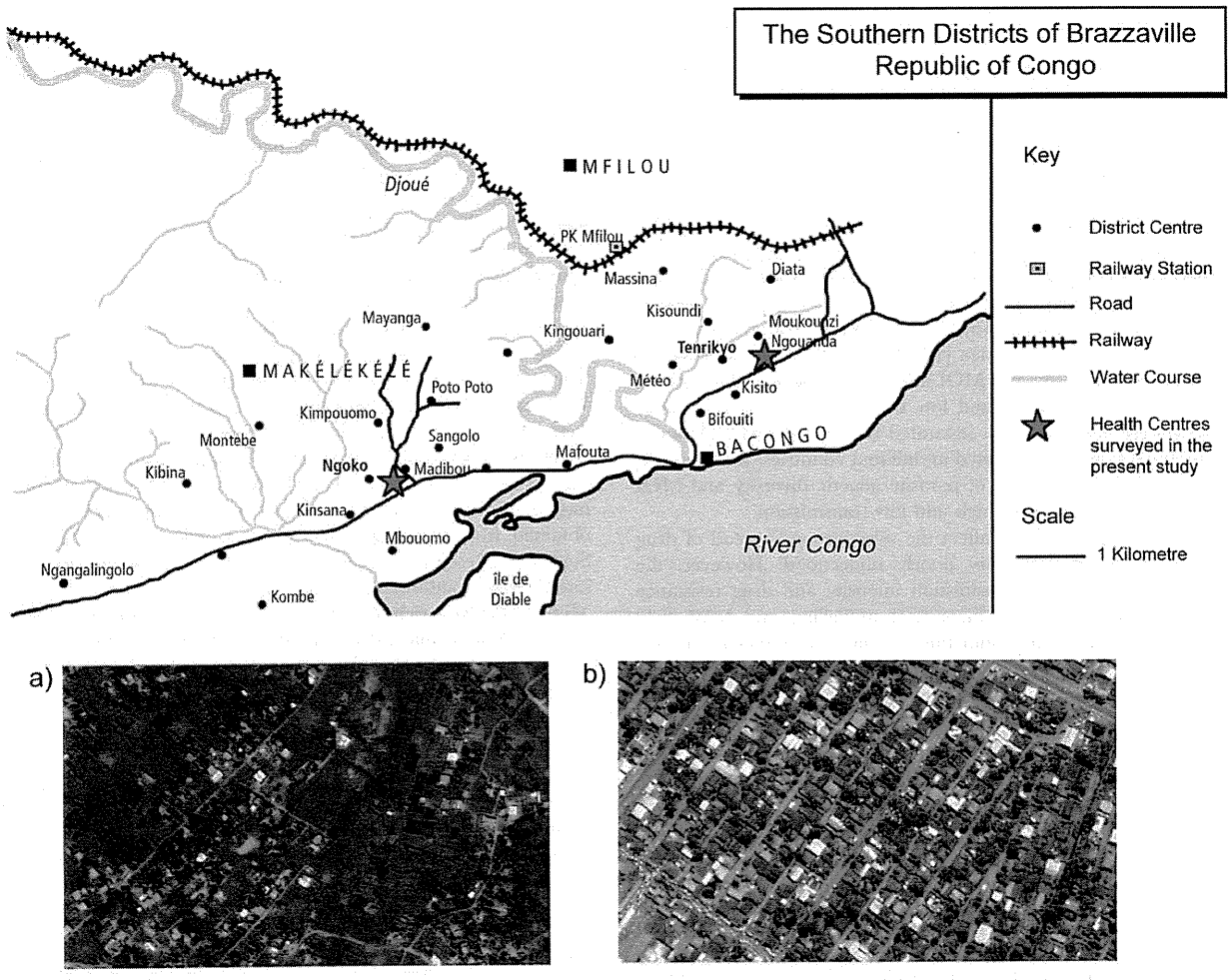

Figure 1. Map of the study area in Brazzaville, Republic of Congo. Blood sample donors were recruited from two health centres, Madibou, which serves patients from the peri-urban area to the west of the Djoue river, and Tenrikyo, which predominantly serves those resident in the urban area to the east of the Djoue. Both centres are marked with a star symbol. Insets (a) and (b) show aerial photographs typical of the regions in which patients from the peri-urban (a) and urban (b) areas reside.
doi:10.1371/journal.pone.0023430.g001

year [40]) and hyper-endemicity (parasite prevalences of >80%, as determined by active case detection of school children resident in the peri-urban area of Makélékélé [39]). Although these entomological inoculation rates and parasite prevalences were determined 20 years prior to the present study, they fit well with the data presented in the present work (see parasite prevalence in the results section), and with those published in 2008 [41].

Parasite DNA extraction from blood spots

For the malaria parasite 18s RNA gene species identification PCR performed in order to detect and species-type malaria parasites, PCR was performed directly on discs cut from the blood sample (according to the manufacturer's instructions), for those samples from Madibou and Tenrikyo health centers that were collected on Whatman® FTA® cards. Briefly, a disc of 1.2 mm in diameter was punched from the centre of each dried blood spotted card and washed three times with Whatman® FTA® Purification Reagent, and twice with TE buffer. This treated disc was then used directly in subsequent PCR analyses. Subsequently, for all further PCR and sequencing analyses, DNA was extracted from the remaining blood spot using an EZ1 BioRobot™ (QIAGEN, Hilden, Germany) according to the manufacturer's instructions. For samples from Pointe-Noire and Gamboma collected on Whatman® 31ETCHR filter paper, DNA extraction was performed using the EZ1 BioRobot™ (QIAGEN, Hilden, Germany) as above.

Species typing PCR

In order to detect the presence of malaria parasites in the samples, and to determine which species of parasites were present, a nested PCR was performed targeting the malaria parasite 18s RNA gene, as previously described [42]. This analysis was performed for all 647 samples. We estimate that the maximum sensitivity of our PCR assay was one parasite per µl of blood.

Correlation between microscopy and PCR

The correlation between the PCR diagnosis and that achieved by thick smear microscopy on site was performed using Kappa coefficient analysis for all samples from Brazzaville. Sub-microscopic

parasite carriers were identified as those individuals deemed negative by miscroscopy, but with positive PCR results.

Typing of MSP1 blocks 2, 4a, 4b, and 6

P. falciparum msp1 may be divided into 17 distinct blocks. We typed four of these blocks; blocks 4a 4b and 6, which are dimorphic, and block 2, which is trimorphic. There are, therefore, 24 possible haplotype combinations for these four blocks. We typed 61 isolates from the peri-urban area, and 41 isolates from the urban area at these four blocks using a PCR protocol which involves the use of primers specific for each allelic type, as previously described [43]. Briefly, forward and reverse primers corresponding to allelic type specific- and inter-allele conserved sequences in blocks 2, 3, 4a, 4b, 5 and 6 were used to differentiate all possible 24 allelic haplotypes covering variable blocks 2, 4a, 4b and 6. Following amplification of blocks 2 to 6, nested PCR was performed to determine allelic types in blocks 4a and 4b. TaKaRa LA Taq^{TM} polymerase (Takara, Japan) was used for amplification of block 2–6, and AmpliTaq Gold® polymerase (Applied Biosystems, USA) for typing of other blocks. PCR products were visualized under UV transillumination following electrophoresis on 2agarose gels stained with ethidium bromide. This allowed us to estimate the minimum number of clones per infection (multiplicity of infection (MOI)), as well as providing data on the diversity of MSP1 within these populations. We also performed this analysis for 23 samples from Pointe-Noire and 27 samples from Gamboma for comparison to the Brazzaville population.

Sequencing of *crt* and *dhfr* genes

Mutations associated with parasite drug resistance to pyrimethamine and chloroquine were assessed by direct sequencing of the *dhfr* and *crt* genes respectively. *dhfr* alleles were determined for 46 and 54 of the samples from the urban and peri-urban areas respectively. *crt* alleles were determined for 37 (urban) and 46 (peri-urban) of the samples. We also sequenced the *dhfr* gene for 24 of the samples from Pointe-Noire and 23 of the samples from Gamboma for comparison to the Brazzaville population. PCR amplification of gene fragments containing point mutations associated with drug resistance was performed for each gene as previously described [44]. For *dhfr*, mutations were assessed at amino acid positions 51, 59, 108 and 164. For *crt*, mutations at amino acid positions 72, 73, 74, 75 and 76 were assessed. Mixed infections were identified in those samples that had double peaks at the relevant nucleotide mutation sites as assessed by visualization of electropherogram peaks following sequencing. In order to meet our criterion for a mixed infection, minor peaks were ignored if they were less than 10% the peak height of the major peak.

Estimation of allele frequencies of *crt* and *dhfr*

In order to estimate allele frequencies for *crt* and *dhfr* wild type and mutant alleles, we utilized the computer program MalHaploFreq [45]. This program allows the estimation of allele frequencies from prevalence data. As high numbers of mixed infections are associated with areas of high transmission, the prevalences of mutant and wild type alleles in a population of samples may not accurately reflect the true frequencies of these alleles in the parasite population. The program uses a maximum likelihood algorithm to estimate allele frequencies based on prevalence data combined with the number of clones per sample (MOI, which we determined by haplotyping *msp1*). In order to assess the statistical significance of allele frequencies between the urban and peri-urban areas, likelihood ratio tests were performed for each area separately, and for the combined data set. The likelihood ratio statistic was then computed as being twice the difference of the sum of the log-likelihoods from the independent likelihood ratio tests and the log-likelihood of the combined data set.

Analysis of eight putatively neutral microsatellite markers

To assess the population structure of the parasite population(s) considered here, and to determine whether parasites from the urban and peri-urban areas were in panmixia, eight putatively neutral microsatellite markers were typed for 41 samples from the urban area, and 39 from the peri-urban area. The microsatellite marker names, accession numbers, whether they are located within coding regions or non-coding regions, and chromosomal locations are summarized in Table 1. Analysis was performed according to Greenhouse *et al.* (2006)[46] or Anderson *et al* (1999)[47], depending on the marker. Briefly, one primer was labeled at the 5' end with either a HEX or 6-FAM fluorophore for detection in Applied Biosystems 3730 DNA Analyzer with GeneMapper Software (Applied Biosystems). The loci of TA81, Poly alpha, TA53, TA43 and TA17 were analyzed by semi-nested PCR using primers of Anderson *et al* (1999). For TA40, TA60 and PfPK2, primers were as designed by Greenhouse *et al* (2006) for single-round PCR. In case of PfPK2, the Greenhouse *et al* primer pair was used in the second round of a nested PCR following initial amplification with the primers of Anderson *et al* (2006).

Population genetic analyses and statistical treatments

Parametric statistical tests were used when data were shown to be normally distributed according to Anderson-Darling tests for normality. In the case of non-normally distributed data, non-parametric tests were used. The statistical significance of differences in parasite prevalence and the proportion of sub-microscopic carriers between areas were tested using Chi-squared tests with Yates' correction for data sets less than 10. The statistical significance of differences in MOI between areas, as determined by *msp1* haplotyping, was analyzed using Mann-Whitney U-tests. The mean ages of patients carrying sub-microscopic parasite infections, and the mean parasite density of patients from the two areas were compared using Student's two-tailed t-tests. These tests were performed using MINITAB® software v15 (LEAD Technologies, Inc., UK). The haplotype diversity index (h) for *msp1* for parasites from the urban and peri-urban areas was calculated using the formula $h = \{n/(n-1)\}\ 5\{1-\sum pi^2\}$ (Nei, 1987) where p and i are the frequency and number of *msp1* haplotypes, respectively. The variance (V) of h was calculated using the formula $V = \{2/n(n-1)\}[2(n-2)\{\sum pi^3 - (\sum pi^2)^2\} + \sum pi^2 - (\sum pi^2)^2]$ [43]. Statistical differences between values of h for *msp1* were determined by Student's two-tailed t-tests. This method was also applied to determine h for each of the eight microsatellite markers. To quantify the pairwise similarity of haplotype pattern between two sites, percent similarity (Ps) was calculated as:

$$Ps = \{SIGMA\_for\_i\}\ [\ Minimum\ (PiA, PiB)]$$

where PiA and PiB are frequency of ith haplotype in Site A and Site B, respectively. The statistical significance of Ps was evaluated by comparing observed Ps to that calculated for randomly mixed samples by 2000 permutations. Percent rank (from the smallest) of the observed value among the 2000 permutation results was used as one-tailed P-value. Linkage disequilibrium within the urban and peri-urban populations was measured using LIAN v3.5 [48]. This program computes the standardized index of association (I^S_A), a measure of haplotype-wide linkage [49]; *P*-values were determined by a Monte Carlo simulation process, with 100,000 iterations. Only those samples for which a complete set of microsatellite alleles were scored were used for this analysis. Genetic differen-

Table 1. Microsatellite markers used in this study. *h* = haplotypes diversity index, *P*-values determined by t-tests.

Microsatellite marker	Chromosome	Accession number	*h* (urban)	*h* (peri-urban)	*P*-value	*Ps (p-value) Urban Vs Peri-urban*
Poly-α	4	LI8785	0.894	0.913	0.55	0.70 (0.60)
TA81	5	AF010510	0.853	0.856	0.98	0.64 (0.19)
TA40	10	AF010542	0.925	0.942	0.75	0.55 (0.37)
PK2	12	X63648	0.879	0.903	0.85	0.72 (0.43)
TA60	13	AF010556	0.837	0.878	0.63	0.71 (0.46)
TA43	14	AF010544	0.931	0.923	0.73	0.64 (0.40)
TA53	9	AF010552	0.664	0.583	0.32	0.80 (0.24)
TA17	8	AF010531	0.822	0.844	0.64	0.70 (0.24)

Ps = percentage similarity, percent rank (from the smallest) of the observed value among 2000 permutation results was used as a one-tailed P-value.
doi:10.1371/journal.pone.0023430.t001

tiation between populations based on the microsatellite data set was measured by calculating values of F_{ST}, carried out using FSTAT v.2.9.4 [50,51]. *P*-values for F_{ST} were calculated by running 10,000 randomizations in a population differentiation test assuming random mating within populations. FSTAT v.2.9.4 was also used to search for linkage disequilibrium between pairs of microsatellite loci for each area. The majority of our samples contained multiple alleles at numerous loci. For the F_{ST} and linkage disequilibrium analyses, the major allele at each locus (in the case of multi-clonal infections) was designated the "major" allele, and haplotypes were constructed using these alleles only, as this approach has previously been shown to give very similar results to comparisons of data sets in which multiple infections are removed [52]. The effective populations sizes of the parasite population from the urban and peri-urban areas was determined using an infinite alleles model where population size (N_e) is determined by the relationship $N_e\mu = h/4(1 - h)$, where μ, the mutation rate, was taken as $1.59\ 5\ 10^{-4}$ (95% confidence interval: $6.98\ 510^{-5}$, $3.7\ 5\ 10^{-4}$), as calculated by Anderson *et al* (2000) from work previously conducted in which the progeny of a laboratory cross of *P. falciparum* were typed with large numbers of microsatellite markers, and the frequency of non-inherited markers scored [53].

Results

Clinical differences between malaria patients from urban and peri-urban areas

There were no significant differences in the ages or sex of patients presenting to either health center, regardless of their area of residence. There were clear differences in parasite prevalences between those patients residing in the urban areas, and those residing the peri-urban area (Table 2). By microscopy, 37% of patients presenting to either health center or who were resident in the urban area were positive for *P. falciparum*, compared to 59% of those resident in the peri-urban regions. When PCR diagnosis was performed, these percentages rose to 42% *P. falciparum* positive for the urban residents, and 75% positive for the peri-urban residents. The correlation between microscopy and PCR were assessed using Kappa co-efficient tests, which revealed a substantial correlation for peri-urban residents (K = 0.71; 95% confidence interval (CI), 0.61–0.81) and an almost perfect correlation for urban residents (K = 0.87; 95% CI, 0.79–0.95), indicating a larger percentage of sub-microscopic parasite carriers in the peri-urban region (20% of all *P. falciparum* cases were sub-microscopic in the peri-urban area, compared with 11% in the urban area, $p<0.001$, (chi-squared test, with Yate's correction). Combining both areas, the mean age of sub-microscopic parasite carriers was significantly higher (15.9 years old) than that of patients with microscopically detectable parasitaemia (8.6 years old) (Student's two-tailed t-test, $P = 0.003$, d.f. = 167), indicative of an age-associated acquisition of immunity. The mean age of sub-microscopic parasite carriers in the urban area was 21.0 years old compared to 15.4 years old in the peri-urban area, but this was not significantly different (Student's two-tailed t-test, $P = 0.42$, d.f. = 12). The mean parasite density of those patients positive by microscopy presenting to the two health centers was 80,206 parasites per microlitre of blood for peri-urban residents, and 31,766 parasites per microlitre for urban residents, a statistically significant difference (Student's two-tailed t-test, $P = 0.048$ d.f. = 104). There was no significant difference between the body temperatures of microscopically malaria positive patients from either area (Table 2).

Drug usage amongst febrile patients from the urban and peri-urban regions

At the time of admittance to either of the health centers, patients with febrile symptoms were asked to provide details of any anti-malarial drugs they had taken following the appearance of symptoms. 25.4% of febrile patients residing in the urban area had taken some form of anti-malarial treatment compared to 19.7% of the residents of the peri-urban region. There were no differences in the types of anti-malarial drugs taken by patients from either area, with the exception of quinine use, which was more commonly used in the peri-urban area than in the urban area (Table 3).

Multiplicity of infection as assessed by msp1 haplotyping and microsatellite analysis

The number of clones per infection was determined for 61 patients resident in the peri-urban area, and 42 patients from the urban area by assessing the numbers of individual *msp1* haplotypes by PCR (Figure 2). The mean number of *msp1* haplotypes per infection for urban residents was 2.21 (95% CI = 1.86–2.56) compared to 2.34 (95% CI = 1.94–2.74) for those resident in peri-urban area (Mann-Whitney test, $P = 0.84$). However, the maximum number of distinct haplotypes per patient was eight for peri-urban residents and five for urban residents. Multiplicities of infections (MOI) were also determined using microsatellite markers, where multiple infections were scored when more than one peak was observed for any of the eight markers assayed for each infection. The MOI for urban residents was 2.11 by this method (compared to

Table 2. Clinical and Entomological data for both the urban and peri-urban regions.

Area	Urban	Peri-urban	Statistical significance
Entomological Inoculation Rate (EIR)[1]	2–12 ib/p/a	50 ib/p/a	ND
Percentage of parasite positive patients infected with;			
P.falciparum	100%	100%	ND
P.vivax	0.0%	0.0%	ND
P.malariae	0.0%	2.9%	ND
P.ovale	0.0%	0.7%	ND
Parasite prevalence (microscopy)[2]	37%	59%	$p<0.001$
Parasite prevalence (PCR)[2]	42%	75%	$p<0.001$
Sub-microscopic positive patients[2]	11%	20%	$p<0.001$
Mean age of sub-microscopic parasite carriers[3]	20.0 yr.	15.4 yr.	$p=0.048$
Mean parasite density at the time of admittance[3, 4]	31,766/μL	80,206/μL	$p=0.048$
Mean body temperature at the time of admittance[3, 4]	37.4°C	37.6°C	NS

[1]data from Trape & Zoulani (1987).
[2]*p*-values determined with chi-squared tests with Yate's correction.
[3]*p*-values determined with student's two-tailed t-tests.
[4]considers only those patients with parasitaemias detectable by microscopy.
ND = Not Determined, NS = Not Significant.
doi:10.1371/journal.pone.0023430.t002

2.17 by *msp1* haplotyping for the same subset of samples), and 1.86 (2.04 by *msp1*) for the peri-urban residents. The strength of agreement between the two methods were assessed using weighted Kappa co-efficient analyses [54], which revealed a "fair" agreement (K = 0.22) between the methods.

Evaluation of parasite genetic diversity between the urban and suburban areas based on msp1 typing

In order to assess the degree of parasite genetic diversity between urban and peri-urban areas, and so determine whether there is a correlation with entomological inoculation rate, we compared the number and types of parasites carrying different haplotypes of the *msp1* gene (Figure 3 panels A and B). We found that there was no significant difference in haplotype diversity (h) between the two regions (peri-urban region, $h = 0.87$, standard error (SE) = 0.01; urban area, $h = 0.88$, SE = 0.02, Student's two-tailed t-test, $P = 0.81$, d.f = 159). Furthermore, we found that there was no significant difference in the genetic *structure* of the two populations; the percent similarity (Ps) of *msp1* haplotypes between the urban and peri-urban regions was 0.84, which did not differ from expectation given random mixing between the two sites (95% range of permutation, 0.73–0.88), suggesting that the same parasite population is shared between the two areas. In order to assess whether *msp1* is a valid marker for population genetic structure that may indicate whether populations are discrete or mixed, we assessed the *msp1* genetic structure for two further sites within the Republic Of Congo, for which it was assumed that there is no parasite population mixing due to geographical isolation. These sites were Pointe-Noire (380 kilometers West of Brazzaville), and Gamboma (250 km to the North of Brazzaville). As there were no parasite population genetic structure differences

Table 3. Drug usage amongst all febrile patients from the urban and peri-urban regions presenting at health centers.

Area	Urban	Peri-urban
Percentage of patients taking malaria drugs	19.7%	25.4%
Percentage of Anti-malarial drugs taken by patients		
Chloroquine	58.8%	54.2%
Sulfadoxine-Pyrimethamine	8.85%	6.3%
Artemether	2.9%	4.2%
Amodiaquine	11.8%	10.4%
Quinine	8.9%	27.0%
Artemsinin and piperaquine combination	2.9%	0.0%
Unknown	8.9%	0.0%

doi:10.1371/journal.pone.0023430.t003

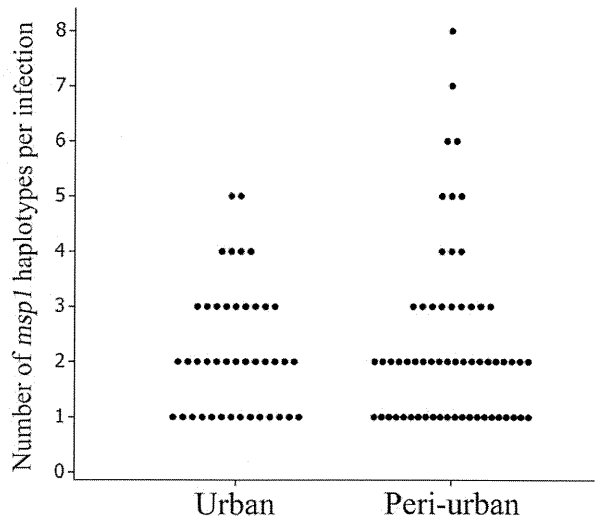

Figure 2. Multiplicities of infections (MOI) for the urban (n = 42) and peri-urban (n = 61) areas as assessed by *msp1* haplotyping.
doi:10.1371/journal.pone.0023430.g002